The 2012 IEEE/ASME International Conference on
Advanced Intelligent Mechatronics
July 11-14, 2012, Kaohsiung, Taiwan

Motion Control of Electric Vehicles Based on Robust Lateral Tire Force Control Using Lateral Tire Force Sensors

Kanghyun Nam, *Student Member, IEEE,* Hiroshi Fujimoto, *Member, IEEE,* and Yoichi Hori, *Fellow, IEEE*

***Abstract*—This paper proposes a new motion control method based on robust lateral tire force control. Since the lateral tire force measurements are available by using multi-sensing hub (MSHub) units which are invented by NSK Ltd, direct lateral tire force control is realizable via active front steering. In control design, robust control method, e.g., 2-degree-of-freedom control (2-DOF) with disturbance observer (DOB), is used for improving the lateral tire force tracking. The proposed motion controller is implemented on an experimental in-wheel-motor-driven electric vehicle and its control performance and effectiveness are verified through experimental results. Finally, practical applications of lateral tire force sensors to vehicle motion control systems are discussed.**

I. INTRODUCTION

DUE to the increasing concerns about motion control of electric vehicles with in-wheel motors, a great deal of research on dynamics control for electric vehicles has been carried out [1], [2]. In order to stabilize the vehicle motion, independent in-wheel motor control and active steering control are treated in previous literatures [3]–[6]. In recent years, integrated control of steering and in-wheel motor has received a lot of intention [3]. In this study, motion stabilization of electric vehicles based on active front steering control is treated. In [5], [6], the yaw stability controllers, which are realized via active front steering by steer-by-wire system, are designed and effectiveness of those controllers is verified through hardware-in-the-loop simulation and experiments, respectively.

As the vehicle motion is governed by the forces generated between tires and road, real-time knowledge of the tire forces is very important when predicting vehicle motion and thereby real-time methods for tire-road forces estimation have been studied [10]. Fortunately, novel lateral tire force sensors, e.g., MSHub units [14], have recently invented by NSK Ltd. and are now under development for practical applications to vehicle motion control systems in the near future. In authors' previous research [7], [8], novel methods for vehicle sideslip angle and roll angle estimation, which are based on lateral tire force sensors, have been proposed and experimentally validated.

In this paper, a new motion control scheme based on robust lateral tire force control is presented. In order to improve the tracking ability of lateral tire force controller, a DOB-based 2-DOF control method is used and active front steering control is utilized for the realization of control law. Moreover, the stability of closed-loop control system is proven by using the small gain theorem. Control performances and effectiveness of the proposed controller are verified through experiments. The proposal of new motion controller based on direct lateral tire force control and its experimental verification are important contributions of this paper.

K. Nam is with the Department of Electrical Engineering, Graduate School of Engineering, The University of Tokyo, Tokyo 113-8656, Japan nam@hori.k.u-tokyo.ac.jp

H. Fujimoto and Y. Hori are with the Department of Advanced Energy, Graduate School of Frontier Sciences, The University of Tokyo, Chiba 277-8561, Japan fujimoto@k.u-tokyo.ac.jp; hori@k.u-tokyo.ac.jp

II. VEHICLE MODEL

In this section, a yaw plane model is introduced to describe the vehicle dynamic behavior. The yaw plane representation is shown in Fig. 1.

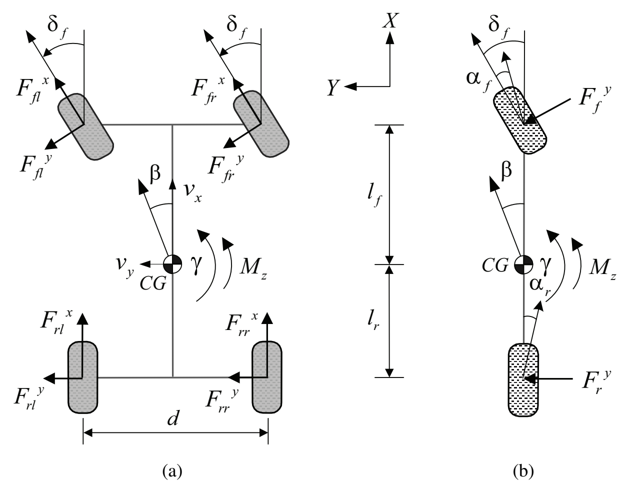

Fig. 1. Planar vehicle model: (a) Four wheel model. (b) Single track model (i.e., bicycle model).

The governing equations for lateral and yaw motions are given by

$$ma_y = mv_x(\dot{\beta}+\gamma) = F_r^y + F_f^x \sin\delta_f + F_f^y \cos\delta_f \quad (1)$$

$$I_z\dot{\gamma} = l_f F_f^x \sin\delta_f + l_f F_f^y \cos\delta_f - l_r F_r^y + M_z \quad (2)$$

where δ_f is a front steering angle, γ is the yaw rate, a_y is the lateral acceleration, β is the vehicle sideslip angle, γ is the yaw rate, v_x is the longitudinal vehicle velocity, I_z is the yaw moment of inertia, l_f and l_r are the distances from center of gravity (CG) to front axle and rear axle, respectively, the front longitudinal tire force F_f^x is the sum of the front left and right longitudinal tire forces (i.e., $F_f^x = F_{fl}^x + F_{fr}^x$), front lateral tire force F_f^y is the sum of the front left and right lateral tire forces (i.e., $F_f^y = F_{fl}^y + F_{fr}^y$), rear lateral tire force F_r^y is the sum of the rear left and right lateral tire forces (i.e.,

$F_r^y = F_{rl}^y + F_{rr}^y$), M_z indicates a direct yaw moment control input, which is generated by the independent torque control of in-wheel motors.

III. Lateral Tire Force Model

A. Lateral Tire Force Model

The tires, which generate longitudinal, lateral forces and moments, have a significant effect on the dynamic characteristics of vehicles. These tire forces are explained by complex relation between tire-road friction, normal force on the tire, variable slip angles, and elastic tire properties. In order to model the tire force generation, several tire models have been developed. A widely used empirical tire model (e.g., magic formula tire model) is dominantly based on empirical formulations deriving from tire test data and a large number of tire parameters. Hence, it is not suitable for real-time application to vehicle control systems. To avoid complex calculation and using tire test data, In this paper, we use linearized tire force model. It should be noted that the lateral tire forces can be linearly approximated for small tire slip angles and are given as

$$F_f^y = -2C_f\left(\beta + \frac{\gamma l_f}{v_x} - \delta_f\right) \quad (3)$$

$$F_r^y = -2C_r\left(\beta - \frac{\gamma l_r}{v_x}\right) \quad (4)$$

where C_f, C_r are the tire cornering stiffnesses of front and rear tires. In order to account for transient behavior of tires, a typical dynamic model, which is the first order dynamics, is used and expressed as follows [12]:

$$\tau_{lag,i}\dot{F}_i^y + F_i^y = \bar{F}_i{}^y \quad (5)$$

where $\tau_{lag,i}$ is the relaxation time constant and calculated from the longitudinal vehicle velocity and tire relaxation length, which is the approximate distance needed to build up tire forces, and $\bar{F}_i{}^y$ is the lateral tire force from a linear tire model described in (3), (4). Based on (3)–(5), the dynamic lateral tire force models for front and rear tires are obtained as follows:

$$\dot{F}_f^y = -\frac{1}{\tau_{lag,f}}F_f^y - \frac{2C_f}{\tau_{lag,f}}\beta - \frac{2l_fC_f}{\tau_{lag,f}v_x}\gamma + \frac{2C_f}{\tau_{lag,f}}\delta_f \quad (6)$$

$$\dot{F}_r^y = -\frac{1}{\tau_{lag,r}}F_r^y - \frac{2C_r}{\tau_{lag,r}}\beta + \frac{2l_rC_r}{\tau_{lag,r}v_x}\gamma \quad (7)$$

where $\tau_{lag,f}$ and $\tau_{lag,r}$ are the relaxation time constants for front and rear tires, respectively.

B. Lateral Tire Force Sensor

In authors' previous literature [7]–[9], cost-effective lateral tire force sensors, called MSHub units shown in Fig. 2, are introduced and used for vehicle state estimation. Lateral tire forces are directly measured by MSHub units which were invented by NSK Ltd. and are now under development for practical applications to vehicle motion control systems in the near future. In many conventional vehicles, wheel hub units with built-in active ABS sensors (i.e., wheel velocity sensor) were equipped. Comparing MSHub units with wheel hub units which are currently used in vehicles, MSHub units have almost the same mechanical structure except for rolling elements in a pair of rows and is capable of being constructed at a low cost. The measurement principle is as follows: the revolution speeds of rolling elements in a pair of rows are sensed by a pair of revolution speed sensors and difference of sensed revolution speeds is used to calculate the radial or axial loads [14]. As shown in Fig. 2, a MSHub unit is installed on rotational axis of the wheel. Through novel load measuring techniques invented by NSK Ltd., the accurate lateral tire force measurements can be realizable without much additional cost.

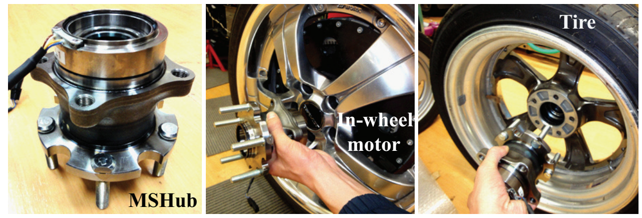

Fig. 2. Real view of lateral tire force sensor (MSHub unit of NSK Ltd.).

Although, by using lateral tire force sensors, a slight increase in sensor price is expected, this kind of cost-effective sensors can provide novel solutions in problems with vehicle state estimation and motion control.

IV. Motion Control Based on Robust Lateral Tire Force Control

The main objective of the motion control system is to provide safety and stability in all driving regions and in the presence of undesirable external conditions such as strong wind or changing tire-road conditions. In this study, a novel motion controller based on direct lateral tire force control is proposed and it is realized via active front steering system. Since the vehicle motion is dominantly governed by forces acting on tires, the motion control based on tire force controls can contribute to improvement of handling and safety performances.

A. Design of Robust Lateral Tire Force Controller

Fig. 3 illustrates the block diagram of the proposed motion controller. The overall control scheme in Fig. 3 is as follows.

1) First, the desired front lateral tire force is obtained from a linear vehicle model and driver's commands such as a steering angle and vehicle speed.
2) Second, the 2-DOF controller is designed based on the defined nominal model for improving the tracking performances.
3) Third, the DOB is designed to compensate for model variations caused by variation of vehicle speed and tire parameters, and reject undesired disturbances. DOB makes the complicated tire force dynamics behave as a defined nominal model [13].

The proposed motion controller is composed of following subsystems.

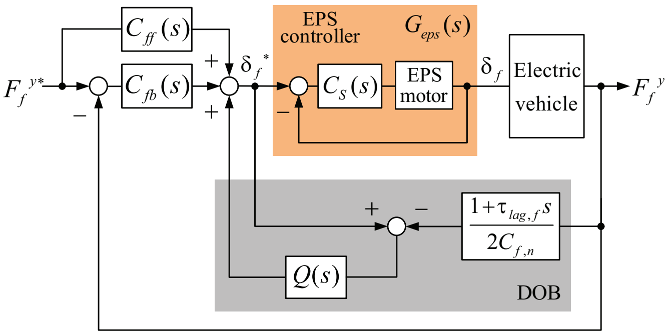

Fig. 3. Block diagram of the lateral tire force controller based on DOB: it is noted that an inner closed loop of the EPS controller $G_{eps}(s)$ has a fast dynamics compared with the vehicle dynamics and thereby its dynamics is not considered in DOB design.

1) Design of Nominal Model: The dynamic lateral force model for front tires is used for control design. It should be note that the lateral tire forces developed at the tire-road contact patch is expressed as a function of tire slip angles and the tire slip angles depend on the vehicle sideslip angle, yaw rate, longitudinal vehicle velocity, and steering angle. In this study, the active steering control is available and it is considered as an only controllable input. Thus, we can obtain a dynamic lateral tire force model which is single-input and single-output (SISO) system as follows:

$$\dot{F}_f^y = -\frac{1}{\tau_{lag,f}}F_f^y - \frac{2C_f}{\tau_{lag,f}}\beta - \frac{2l_fC_f}{\tau_{lag,f}v_x}\gamma + \frac{2C_f}{\tau_{lag,f}}\delta_f \quad (8)$$

Here, the tire forces generated by the influences of β and γ are considered as disturbances and thereby it is rewritten as

$$\dot{F}_f^y = -\frac{1}{\tau_{lag,f}}F_f^y + \frac{2C_{fn}}{\tau_{lag,f}}\delta_f + F_d^y \quad (9)$$

where F_d^y indicates lumped lateral force disturbances, which include the influences of β, γ, and other external forces ΔF^y like side wind force, and it is expressed as follows:

$$F_d^y = -\frac{2C_f}{\tau_{lag,f}}\left(\beta + \frac{l_f\gamma}{v_x}\right) + \Delta F^y. \quad (10)$$

From (9), a transfer function for the nominal lateral tire force model is obtained as

$$P_n(s) = \frac{F_f^y(s)}{\delta_f(s)} = \frac{2C_{f,n}}{1+\tau_{lag,f}s} \quad (11)$$

where $C_{f,n}$ is a nominal front tire cornering stiffness for a value (i.e., =12500N/rad) on a high–μ road (i.e., μ=0.9), $\tau_{lag,f}$ is a nominal relaxation time constant which is defined as a constant for the certain vehicle speed.

2) Generation of Desired Lateral Tire Force: The objective of the vehicle motion control is to improve the vehicle steadiness and transient response properties, enhancing vehicle handling performance and maintaining stability in those cornering maneuvers, e.g., the yaw rate γ or sideslip angle β of the vehicle should be close to desired vehicle responses (γ_d and β_d). In this study, the advanced motion control method based on direct lateral tire force control has been proposed. This means that lateral tire forces, which the tires generate, should be controlled to follow the desired lateral tire forces $F_f^{y\star}$. Desired vehicle and tire force responses are defined based on driver's cornering intention (e.g., drivers' steering command and vehicle speed). In usual, vehicle responses during steady state cornering, i.e., $\dot{\beta} = \dot{\gamma} = 0$ in (1), (2), are used as desired vehicle responses. Desired vehicle sideslip angle, yaw rate, and front lateral tire force for given steering angle and vehicle speed are defined as

$$\gamma_d = \frac{1}{1+K_sv_x^2}\frac{v_x}{l}\cdot\delta_f, \quad \beta_d = \frac{1-\left(\frac{ml_fv_x^2}{2ll_rC_r}\right)}{1+K_sv_x^2}\frac{l_r}{l}\cdot\delta_f \quad (12)$$

$$F_f^{y\star} = \frac{\omega_f}{s+\omega_f}\left(\frac{I_z}{l_f+l_r}\cdot\dot{\gamma}_d + \frac{mv_x}{l_f+l_r}\cdot(\dot{\beta}_d+\gamma_d)\right) \quad (13)$$

$$K_s = \frac{m(l_rC_r - l_fC_f)}{2l^2C_fC_r} \quad (14)$$

where the desired front lateral tire force $F_f^{y\star}$, described in (13), is obtained from (1), (2), ω_f is the cutoff frequency (e.g., in this paper, 15rad/s is chosen) of a tire force model filter, K_s is the vehicle stability factor, which explains the steering characteristics of the vehicles.

3) Design of 2-DOF Controller: The main objective of proposed control system is to realize the robust tracking control of front lateral tire forces. 2-DOF control methodology is applied to control system design [11]. The 2-DOF controller consists of two compensators, i.e., feed-forward compensator $C_{ff}(s)$ and feedback compensator $C_{fb}(s)$.

The feed-forward compensator $C_{ff}(s)$ is designed as an inverse nominal model, i.e.,

$$C_{ff}(s) = P_n^{-1}(s) = \frac{1+\tau_{lag,f}s}{2C_{f,n}} \quad (15)$$

where $\tau_{lag,f}$ = 0.08 sec and $C_{f,n}$ = 12500 N/rad are used in experiments.

The feedback compensator $C_{fb}(s)$ is designed as a conventional Proportional-Integration (PI) controller as follows:

$$C_{fb}(s) = \frac{K_Ps+K_I}{s} \quad (16)$$

where K_P, K_I are the proportional and integration gains, and these are chosen by pole placement based on the given performance specifications, e.g., tracking error at low frequency: <10%, control bandwidth of closed-loop system: 10rad/sec.

4) Design of Disturbance Observer (DOB): In general, the DOB is used for rejecting disturbance and compensating for variation of plant dynamics by treating the variations as an equivalent disturbances. In this study, the DOB, which is an inner-loop controller, has been used for aforementioned reasons. In the design of DOB, the selection of the low pass filter called a Q-filter $Q(s)$ is very important. It is required to select the $Q(s)$ such that $Q(s)P_n^{-1}(s)$ is realizable. Thus, a first order loss pass filter is used in the proposed control system.

$$Q(s) = \frac{\omega_Q}{s+\omega_Q} \quad (17)$$

where ω_Q is a cutoff frequency of the $Q(s)$ which should be chosen to satisfy the stability condition.

B. Stability Analysis of the Proposed Control System

In this section, the stability of the proposed control system has been discussed. Especially, we have made stability analysis in the presence of multiplicative model uncertainty $\Delta(s)$ in the plant. Note that the vehicle system is subjected to large model variations due to varying parameters such as vehicle speed and tire-road parameters. In order to account for these model variations, a multiplicative model uncertainty $\Delta(s)$ is imposed on the defined nominal model as shown in Fig. 4, i.e.,

$$P(s) \quad = \quad P_n(s)\,(1+\Delta(s)) \tag{18}$$

where $P(s)$ is the actual plant which is the actual relationship between front steering angle δ_f to front lateral tire force F_f^y and it is expressed in the Laplace domain from (8),

$$\begin{aligned} P(s) &= \frac{F_f^y(s)}{\delta_f(s)} \\ &= -\frac{2C_f}{1+\tau_{lag,f}s}\left(G_{\beta\delta_f}(s)+\frac{l_f}{v_x}G_{\gamma\delta_f}(s)-1\right) \end{aligned} \tag{19}$$

where $G_{\beta\delta_f}(s)$ is the transfer function between a front steering angle and a vehicle sideslip angle, $G_{\gamma\delta_f}(s)$ is the transfer function between a front steering angle and a yaw rate. Both transfer functions are obtained from (1) and (2).

Frequency responses of the actual plant are obtained using (19) and varying parameters with bounded values. A parameter set including the bounds of several varying parameters is given by

$$\text{Parameter set:} \begin{cases} C_f \in (5000, 13000),\;\; C_r \in (10000, 32500) \\ v_x \in (5,\;\; 25) \\ \tau_{lag,f} \in (0.05,\;\; 0.25) \end{cases}$$

where the bounds for each parameter are defined by considering the practical vehicle driving range.

From (8), (19), and above parameter set, the multiplicative model uncertainty $\Delta(s)$ is calculated as follows:

$$\Delta(s) \quad = \quad \frac{P(s)-P_n(s)}{P_n(s)}. \tag{20}$$

In order to prove the closed-loop stability against model uncertainty $\Delta(s)$, the small gain theorem is used. In usual,

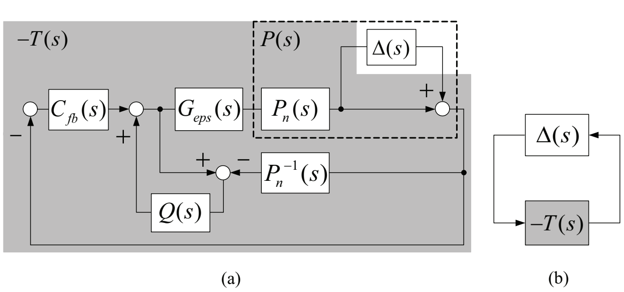

Fig. 4. Block diagram of proposed control system: (a) Block diagram of closed loop control system with multiplicative model uncertainty. (b) Equivalent block diagram.

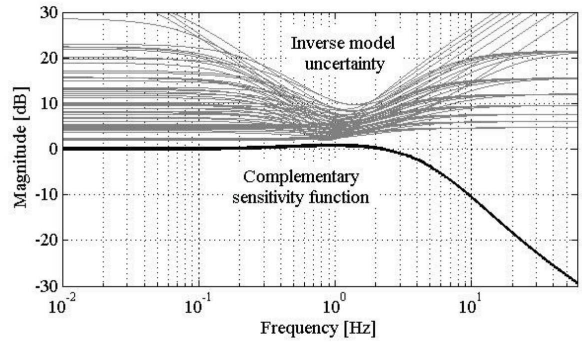

Fig. 5. Frequency magnitude response for small gain theorem check.

the small gain theorem is used as a conservative stability check in cases where there is time-varying model uncertainty. According to the small gain theorem, a sufficient condition for stability is given by

$$|\Delta(j\omega)T(j\omega)|_\infty < \;1 \qquad \text{for all } \omega \in \Re \tag{21}$$

where $T(j\omega)$ is the complementary sensitivity function and described as

$$T(j\omega) \quad = \quad \frac{P_n(j\omega)G_{eps}(j\omega)C_{fb}(j\omega)+Q(j\omega)}{1+P_n(j\omega)G_{eps}(j\omega)C_{fb}(j\omega)}. \tag{22}$$

Note that as long as multiplicative model uncertainty $\Delta(j\omega)$ in the plant satisfies the inequality (21), the stability of close-loop system is guaranteed. This is graphically illustrated in the magnitude Bode plot of Fig. 5. We can confirm that the stability is guaranteed because the inequality (21) is satisfied, that is, magnitude of the complementary sensitivity function is below the magnitude of inverse model uncertainty all over the frequencies.

V. EXPERIMENTAL VERIFICATION

In order to implement the proposed motion controller, an in-wheel-motor-driven electric vehicle (shown in Fig. 6 (a)), which was developed by Hori/Fujimoto research team, was used. Lateral tire force sensors, i.e., MSHub units, are attached in each wheel and an EPS system for realizing active front steering control is available. An EPS motor, shown in Fig. 6(b), is a high speed DC motor with 250W power output. In addition, the dSPACE AutoBox (DS1103), which consists of a power PC 750GX controller board running at 933 MHz, 16 channel A/D converter, and 8 channel D/A converter, are used for real-time data acquisition and control.

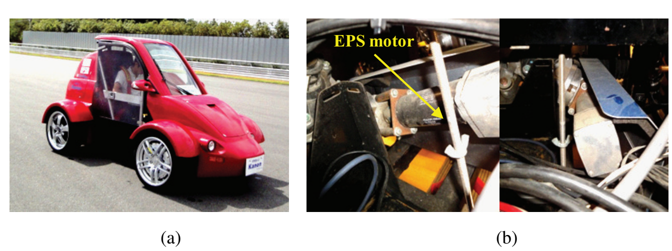

Fig. 6. Real view of an experimental electric vehicle: (a) In-wheel-motor-driven electric vehicle. (b) EPS system.

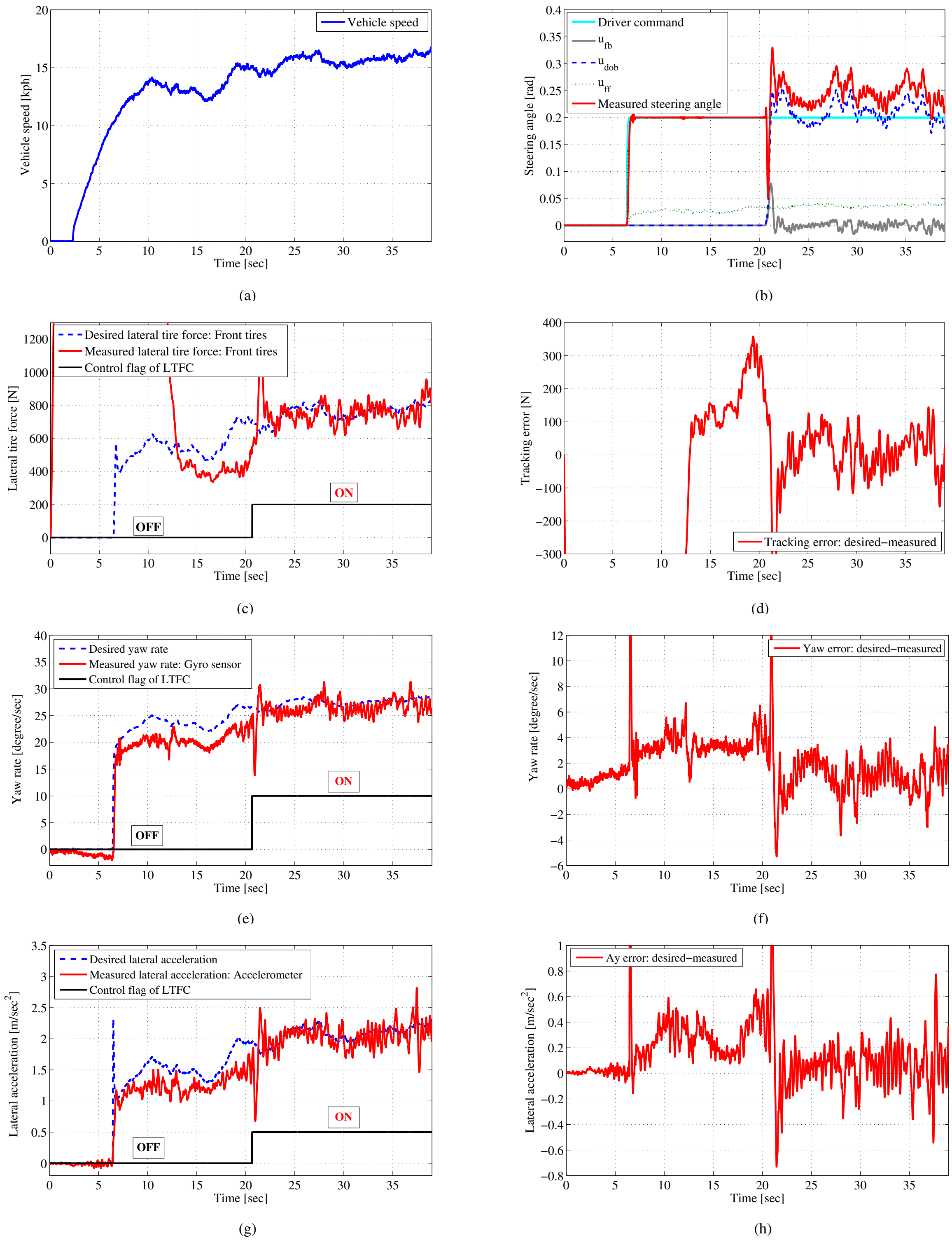

Fig. 7. Experimental results on dry asphalt ($\mu \simeq 0.9$) with gravel ($\mu \simeq 0.5$). (a) Vehicle speed. (b) Control law: steering angle. (c) Lateral tire force. (d) Tracking error. (e) Yaw rate. (f) Yaw rate error. (g) Lateral acceleration. (h) Lateral acceleration error.

To demonstrate the performance and effectiveness of the proposed motion controller, field tests were carried out with following driving conditions; 1) constant vehicle speed; 2) step steering command; 3) a proposed controller begins to work by enabling the manual control switch; 4) front-wheel driving mode. Fig. 7 shows the experimental results for the proposed motion controller. A controller begins to work when the control switch is turned on by a driver. At t=20.7sec, a proposed lateral tire force controller (LTFC) begins to work as shown in Fig. 7 (c). Accordingly, an EPS motor also begun to

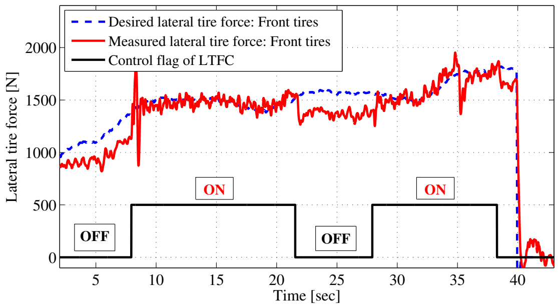

Fig. 8. Result of a field test with v_x = 27 km/h, δ_{cmd} = 0.15 rad, $|a_y|_{\text{max}}$ = 5 m/s^2.

be controlled to realize robust lateral tire force control and its results are shown in Fig. 7 (b). A step steering input has been commanded by a driver at t=6.5sec and an inner-loop EPS motor controller has worked for tracking the driver's steering command. The measured steering angle, which can be seen as a control law, is equal to the sum of the each compensator such as feed-forward/feedback compensators and DOB, i.e., $\delta_f^\star = u_{law} = u_{ff} + u_{fb} + u_{DOB}$. Fig. 7 (c) and (d) represent the results of direct lateral tire force control using lateral tire force sensors. The measured front lateral tire force (i.e., thick red line) is relatively well matched the desired force trajectory (i.e., dotted blue line) while the control flag of LTFC (i.e., thick black line) is ON-state. Fig. 7 (d) shows the tracking error which is defined as a difference between desired value and actual measured value. We can confirm that the tracking error at low frequency is within the specified tracking error limit (i.e., $<10\%$). Although there exist a chattering-like error in experimental results due to sensor accuracy and noise issues in lateral tire force sensors, performances and effectiveness of the proposed motion controller can be verified through results of Fig. 7 (c). In addition, the effectiveness of the proposed motion controller is also verified from the results of vehicle motion sensors including yaw rate sensor and lateral acceleration sensor. Fig. 7 (e), (f) and Fig. 7 (g), (h) represent the yaw rate and lateral acceleration which are measured from Gyro sensor and accelerometer respectively. Even though yaw rate and lateral acceleration of the vehicle are not directly controlled, the measured values are well matched the desired values with small errors. Therefore, a proposed motion controller based on direct front lateral tire force control contributes to stabilization of the vehicle motion. This new motion control scheme based on tire force control is an important contribution of this study.

To verify the effectiveness of a proposed LTFC in the critical driving situation (e.g., severe lateral motion, i.e., $|a_y| > 5$ m/s^2), a step steering test at v_x = 27 km/h has been performed and it result is shown in Fig. 8. The lateral tire force that the vehicle generated followed the desired lateral tire force while the control flag of LTFC was activated.

VI. CONCLUSIONS AND FUTURE WORKS

This paper has presented a new motion control scheme based on robust lateral tire force control. Recently, cost-effective lateral tire force sensors have been invented by NSK Ltd. and are now under development for practical applications to vehicle motion control systems. Considering that the vehicle cornering motion is dominantly governed by lateral forces acting on tires, the motion control based on direct lateral tire force control can contribute to robust stabilization of the vehicle motion. In order to improve the tracking ability of lateral tire force controller, a DOB-based 2-DOF control method is used and active front steering control is utilized for the realization of control law. The stability of the closed-loop control system is proved by using the small gain theorem. Finally, performance and effectiveness of the proposed motion controller are verified through experimental results.

VII. ACKNOWLEDGMENTS

This work was supported in part by the Industrial Technology Research Grant Program from New Energy and Industrial Technology Development Organization (NEDO) of Japan, and by the Ministry of Education, Culture, Sports, Science and Technology under Grant 22246057. The authors would like to thank NSK Ltd. for providing MSHub units and technical support.

REFERENCES

[1] N. Mutoh and Y. Nakano, ''Dynamics of front-and-rear-wheel-independent-drive-type electric vehicles at the time of failure,'' *IEEE Trans. Ind. Electron.*, vol. 59, no. 3, pp. 1488–1499, Mar. 2012.

[2] Y. Chen and J. Wang, ''Fast and global optimal energy-efficient control allocation with applications to over-actuated electric ground vehicles,'' *IEEE Trans. Control Syst. Technol.*, vol. PP, no. 99, pp. 1–10, 2012.

[3] N. Ando and H. Fujimoto, "Yaw-rate control for electric vehicle with active front/rear steering and driving/braking force distribution of rear wheels," *IEEJ Transactions on Industry Applications*, vol. 131, no. 4, pp. 616–623, 2011.

[4] P. Falcone, F. Borrelli, J. Asgari, H.E. Tseng, and D. Hrovat, ''Predictive Active Steering Control for Autonomous Vehicle Systems,'' *IEEE Trans. Control Syst. Technol.*, vol. 15, no. 3, pp. 566–580, May 2007.

[5] B. A. Guvenc, L. Guvenc, and S. Karaman, "Robust yaw stability controller design and hardware-in-the-loop testing for a road vehicle," *IEEE Trans. Veh. Technol.*, vol. 58, no. 2, pp. 555-571, Feb. 2009.

[6] K. Nam, Y. Kim, S. Oh, and Y. Hori, ''Steering angle-disturbance observer(SA-DOB) based yaw stability control for electric vehicles with in-wheel motors,'' in *Proc. of Int. Conf. on Control Automation and Systems (ICCAS),* , pp. 1303–1307, Dec. 2010.

[7] K. Nam, S. Oh, H. Fujimoto, and Y. Hori, "Vehicle state estimation for advanced vehicle motion control using novel lateral tire force sensors", in *American Control Conf.*, Sanfrancisco, pp. 4853–4858, 2011

[8] K. Nam, S. Oh, H. Fujimoto, and Y. Hori, "Estimation of sideslip and roll angles of electric vehicles using lateral tire force sensors through RLS and Kalman filter approaches," *IEEE Trans. Ind. Electron.*, DOI (identifier) 10.1109/TIE.2012.2188874. (To be published)

[9] K. Nam, H. Fujimoto, and Y. Hori, "Lateral stability control of in-wheel-motor-driven electric vehicles based on sideslip angle estimation using lateral tire force sensors," *IEEE Trans. Veh. Technol.*, DOI (identifier) 10.1109/TVT.2012.2191627. (To be published)

[10] M. Doumiati, A. C. Victorino, A. Charara, and D. Lechner, "Onboard real-time estimation of vehicle lateral tire–road forces and sideslip angle," *IEEE/ASME Trans. Mechatron.*, vol. 16, no. 4, pp. 601–614, Aug, 2011.

[11] T. Umeno and Y. Hori, ''Robust speed control of DC servomotors using modern two degrees-of-freedom controller design,'' *IEEE Trans. Ind. Electron.*, vol. 38, no. 5, pp. 363–368, Oct. 1991.

[12] R. Rajamani, *Vehicle Dynamics and Control*. New York: Springer-Verlag, 2005.

[13] A. Sabanovic and K. Ohnishi, *Motion Control Systems*. Wiley-IEEE Press, 2011.

[14] K. Ono, T. Takizawa,and M. Aoki, "Preload measuring device for double row rolling bearing unit," U.S. Patent 20090052825A1, Feb. 26, 2009.